Journal of Alloys and Compounds 522 (2012) 74–77

Contents lists available at SciVerse ScienceDirect

Journal of Alloys and Compounds

journal homepage: www.elsevier.com/locate/jallcom

Synthesis of monoclinic Na_3ScF_6:1 mol% Er^{3+}/2 mol% Yb^{3+} microcrystals by a facile hydrothermal approach

Shuwei Hao, Liang Sun, Guanying Chen*, Hailong Qiu, Chao Xu, Timonah N. Soitah, Yu Sun, Chunhui Yang*

School of Chemical Engineering and Technology, Harbin Institute of Technology, Harbin 150001, People's Republic of China

ARTICLE INFO

Article history:
Received 1 October 2009
Received in revised form 15 January 2012
Accepted 16 January 2012
Available online 28 January 2012

Keywords:
Na_3ScF_6 microcrystal
Luminescence
Upconversion properties

ABSTRACT

For the first time, a facile hydrothermal approach to synthesize the highly efficient 1 mol% Er^{3+}/2 mol% Yb^{3+} codoped Na_3ScF_6 upconversion (UC) microcrystals is reported. The X-ray diffraction (XRD) patterns indicate that the prepared powders possess monoclinic structure. Field emission scanning electron microscopy (FESEM) shows that these samples have monocline morphology with high crystallinity. Under 980 nm diode laser excitation, Na_3ScF_6:1 mol% Er^{3+}, 2 mol% Yb^{3+} microcrystals emit strong green and red upconversion emissions. UC mechanisms for these emissions are proposed based on their pump power dependences.

1. Introduction

Rare-earth-doped upconversion (UC) materials have recently garnered considerable attentions due to their potential applications in solid state lasers [1], 3D volumetric displays [2,3], biological imaging and therapy [4–6], low-intensity near infrared (NIR) conversion [7], photovoltaics [8,9], etc. Photon UC is a unique nonlinear process that converts long-wavelength excitation, usually in the NIR range into visible or ultraviolet (UV) radiations through use of the ladder-like energy levels of rare-earth ions diluted in the host lattice. Among these UC materials, fluoride host materials have intriguing characteristics to distinguish them for these endeavors. For example, fluoride host lattices have high thermal, optical, and chemical stability, and they possess an extremely wide transparent spectroscopic range for light frequency conversion from far infrared to vacuum UV [10,11]. Moreover, they have low phonon cutoff energy that can efficiently decrease multiphonon-assissted nonradiative relaxations in the intermediate states of rare earth ions, therefore, generally leading to the high UC efficiency [12]. Fluoride host materials of $MREF_x$ (M = Li, Na, K) have been demonstrated to possess higher UC luminescence efficiency than the other UC fluoride materials investigated [13–15]. As such, the preparation and controlled synthesis of $MREF_x$ fluoride materials have attracted great interests in the literature [7,15–25]. Micro- and nano-crystals of $NaYF_4$ and $NaGdF_4$ with diverse shapes have been successfully synthesized using various chemical techniques such as, co-precipitation, hydrothermal, solvothermal, thermal decomposition approaches [26–30], etc. Moreover, nano-crystals of $LiYF_4$ have also been synthesized by the thermal decomposition method recently [31]. However, there were no previous reports on the synthesis of Na_3ScF_6 UC materials.

Similar to other $MREF_x$ materials (e.g., $NaYF_4$), Na_3ScF_6 lattice possess excellent optical qualities [32], thus the Na_3ScF_6 is expected to be a promising host lattice. It is known that the UC emission intensity is sensitive to the symmetry and the phonon energy of host lattice, and the lower symmetry of the crystal field and shorter distance between rare-earth ions are beneficial to improve the UC efficiency [33,34]. Ma et al. has shown that the introduction of Sc^{3+} ions in $NaYF_4$:Er^{3+}/Yb^{3+} nanoparticles can remarkably enhance the blue, green, and red upconverted emissions due to the lowering the symmetry of the local crystal field of the $NaYF_4$ host lattice and the shortening of the distance between rare-earth ions [35]. This result suggests that the $NaScF_x$ host lattice might have promising UC properties; however, this conclusion remains unclear up to now due to the lacking of the data in the literature. Herein we report the synthesis of Na_3ScF_6:1 mol% Er^{3+}, 2 mol% Yb^{3+} microcrystals. We then compared their emission UC intensity with $NaYF_4$:1 mol% Er^{3+}, 2 mol% Yb^{3+} microcrystals of the same size. We found that the resulting Na_3ScF_6:1 mol% Er^{3+}, 2 mol% Yb^{3+} microcrystals showed similar intense UC emissions with that of $NaYF_4$:1 mol% Er^{3+}, 2 mol% Yb^{3+} microcrystals. The result here demonstrates that the monoclinic Na_3ScF_6 is also a promising UC host lattice for potential applications.

* Corresponding authors. Tel.: +86 451 86413707; fax: +86 451 86488720.
E-mail addresses: chenguanying@hit.edu.cn (G. Chen), yangchh@hit.edu.cn (C. Yang).

0925-8388/$ – see front matter © 2012 Published by Elsevier B.V.
doi:10.1016/j.jallcom.2012.01.080

2. Experimental description

2.1. Preparation of Na_3ScF_6 microcrystals

Analytical grade chemicals of Sc_2O_3, Yb_2O_3, Er_2O_3, were supplied by (Guangdong Province) CongHua City JianFeng Rare Earth Company. HF, NaOH, HNO_3, EDTA and salicylic acid were purchased from Tianjin Chemical Reagent Company and used as the starting materials without further purification. 0.1381 g of Sc_2O_3 (99.999%), 0.0197 g of Yb_2O_3 (99.999%) and 0.0038 of Er_2O_3 (99.999%) were mixed sufficiently and dissolved in dilute HNO_3 by heating and stirring to prepare the stock solution. The mixed nitrate solution thus was allowed to cool down to room temperature and then 0.584 g of ethylenediaminetetraacetic acid (EDTA) was added into the mixed nitrate solution. After mixing with 2 mL HF (99.9%) until a white homogeneous solution appeared, a well-controlled amount of NaOH (99.9%) solution was added while magnetically stirring until a pH = 4 was reached. The mother solution containing the white suspension was sealed in 50 mL Teflon-lined stainless steel autoclaves which were allowed to react at 180 °C for 12 h. The as-prepared white suspensions were washed with ethanol and deionized water several times and then dried at 80 °C for 2 h.

2.2. Characterization

X-Ray powder diffraction (XRD) pattern was carried out by a Rigaku D/max-γB diffractometer equipped with a rotating anode and a Cu Kα source (λ = 0.15418 nm). FESEM micrographs were obtained using a field emission scanning electron microscope (FESEM, MX2600FE). Upconversion luminescence properties were measured by a regeneratively amplified 980 nm diode laser (Hi-Tech Optoelectronics Co. Ltd., Beijing). The emitted UC fluorescence was collected by a lens-coupled monochromator (Zolix Instruments Co. Ltd., Beijing) of 3 nm spectral resolution with an attached photomultiplier tube (Hamamatsu CR131). All measurements were performed at room temperature, preserving the same geometry for the UC luminescence recording.

3. Results and discussion

Fig. 1 shows the XRD pattern of the as-prepared Na_3ScF_6:1 mol% Er^{3+}, 2 mol% Yb^{3+} powders. It can be seen that the peak positions and intensities of the microcrystals are in good agreement with that in the contrasted standard monoclinic Na_3ScF_6 (space group: $P2_1/n$, JCPDS no. 20-1153). The lattice parameters are calculated to be: (a) 5.602 Å, (b) 5.803 Å, and (c) 8.121 Å. Since there is no other phases displayed in Fig. 1, this demonstrates that Yb^{3+}/Er^{3+} were doped into the Na_3ScF_6 host lattices.

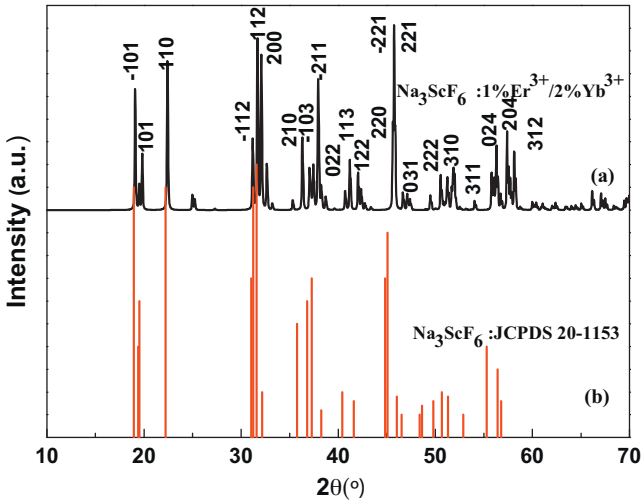

Fig. 1. XRD patterns for the as-prepared: (a) Na_3ScF_6:1 mol% Er^{3+}, 2 mol% Yb^{3+}, and (b) the standard data of monoclinic Na_3ScF_6 (JCPDS no. 20-1153) as a reference.

A low-magnification FESEM image (Fig. 2a) shows that the as-prepared Na_3ScF_6:1 mol% Er^{3+}, 2 mol% Yb^{3+} exhibits monoclinic phase morphology with good uniformity and dispersity, which agrees well with the XRD result in Fig. 1. According to Fig. 2a, the average size of Na_3ScF_6:Er^{3+}/Yb^{3+} powders is calculated to be about 1 μm in length. Fig. 2b–d presents a higher magnification FESEM image of the prepared powders. As can be seen in these images, the Na_3ScF_6:1 mol% Er^{3+}, 2 mol% Yb^{3+} powders show smooth

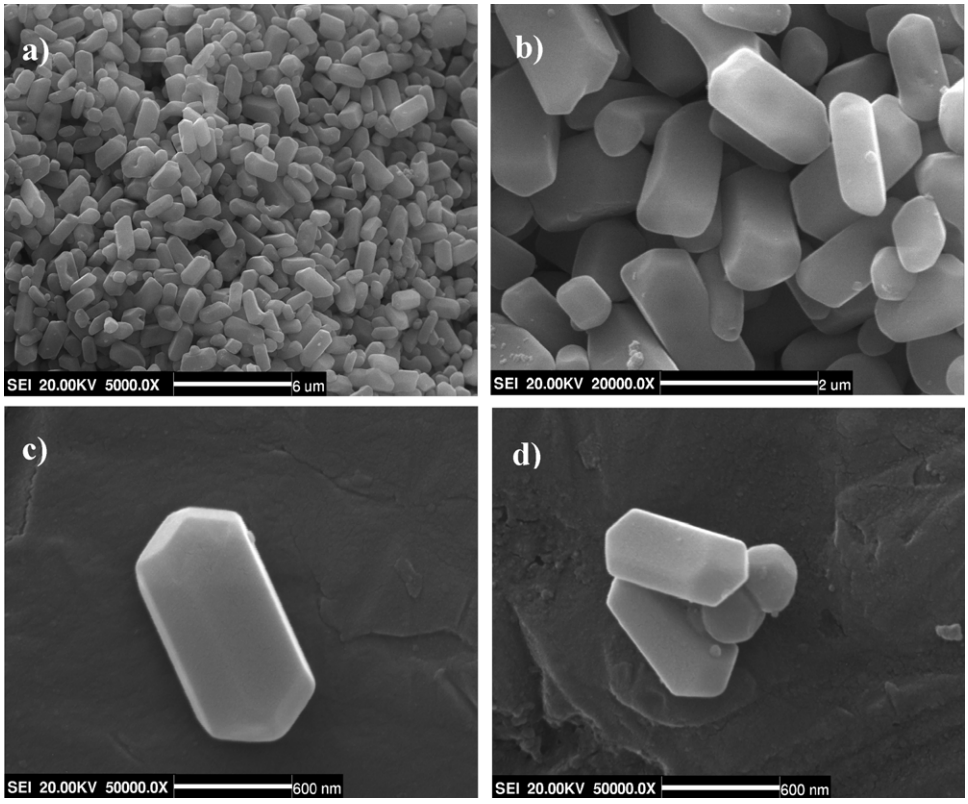

Fig. 2. Typical FESEM images of the Na_3ScF_6:1 mol% Er^{3+}, 2 mol% Yb^{3+}.

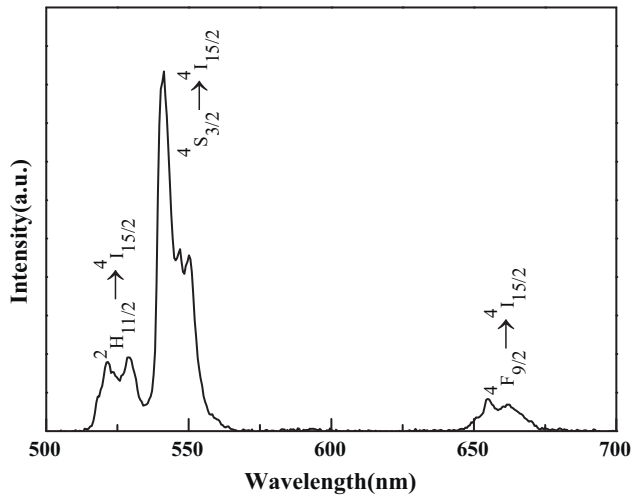

Fig. 3. The UC emission spectra of Na_3ScF_6:1 mol% Er^{3+}, 2 mol% Yb^{3+} microcrystals under 980 nm excitation.

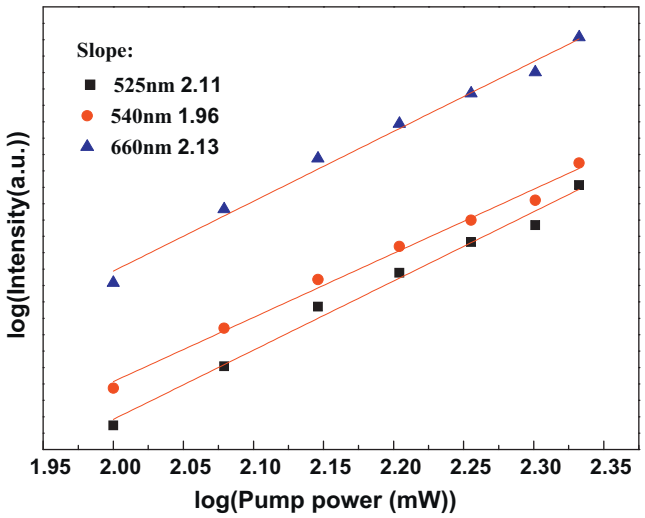

Fig. 5. Dependence of green and red emission from Na_3ScF_6:1 mol% Er^{3+}, 2 mol% Yb^{3+} microcrystals on pumping power.

morphology with perfect crystallization, and their microcrystals possess clear monoclinic morphology.

Fig. 3 shows the UC fluorescence of Na_3ScF_6:1 mol% Er^{3+}, 2 mol% Yb^{3+} microcrystals in the spectroscopic range of 500–700 nm under diode laser excitation of 980 nm. Two UC bands of green and red centered at 525/540 and 660 nm are observed, which can be assigned to the $^2H_{11/2}/^4S_{3/2} \rightarrow {}^4I_{15/2}$ and $^4F_{9/2} \rightarrow {}^4I_{15/2}$ transitions of Er^{3+} ions, respectively. It is worthwhile to mention that a strong green emission was observed in Na_3ScF_6:1 mol% Er^{3+}, 2 mol% Yb^{3+} microcrystals even by the naked eyes.

From Fig. 4, $NaYF_4$:1 mol% Er^{3+}, 2 mol% Yb^{3+} microrods with uniform morphology and high quality were successfully synthesized via the same hydrothermal route. And the size of the as-prepared microrods is close to the Na_3ScF_6:1 mol% Er^{3+}, 2 mol% Yb^{3+} microcrystals. Furthermore, the UC emission intensity of Na_3ScF_6:1 mol% Er^{3+}, 2 mol% Yb^{3+} is compared with that of $NaYF_4$:1 mol% Er^{3+}, 2 mol% Yb^{3+} microrods. As shown in Fig. 4, the strongest peak of $NaYF_4$:1 mol% Er^{3+}, 2 mol% Yb^{3+} microrods, centered at 540 nm, is slightly better than the Na_3ScF_6:1 mol% Er^{3+}, 2 mol% Yb^{3+} microcrystals. However, it should be pointed out that the stronger green emission, comparing with the red emission, was observed in Na_3ScF_6:1 mol% Er^{3+}, 2 mol% Yb^{3+} microcrystals, which could be in favor of obtaining high purity of single-band UC green emission attractive for color display applications [36]. Moreover, the synthesis of Na_3ScF_6 microcrystals has not been reported so far, which indicates the Na_3ScF_6 host matrix can be developed to enhance the emission intensities. Thus it demonstrates that the Na_3ScF_6:1 mol% Er^{3+}, 2 mol% Yb^{3+} microcrystals is also an excellent host lattice for upconversion luminescence materials and should be particularly useful for further development of novel upconversion microcrystals with potentially high emission intensities.

In order to investigate the upconversion mechanism, pump power-dependence of green and red UC emissions was measured and displayed in a logarithmic scale (Fig. 5). For the unsaturated status, the number of photons that are required to populate the upper emitting state can be obtained by the relation $I_f \propto P^n$, where I_f is the fluorescent intensity, P is the pump laser power and n is the number of the laser photons required. From Fig. 4, n = 2.11, 1.96, and 2.13 are obtained for $H_{11/2} \rightarrow {}^4I_{15/2}$, $^4S_{3/2} \rightarrow {}^4I_{15/2}$, and $^4F_{9/2} \rightarrow {}^4I_{15/2}$ transitions, respectively. These values suggest two-photon process is involved to populate the $H_{11/2}$, $^4S_{3/2}$, and $^4F_{9/2}$ state, respectively.

Fig. 6 displays the energy levels of Yb^{3+} and Er^{3+} ions as well as the proposed UC mechanisms. Yb^{3+} ion absorbs one laser photon and is excited from the ground $^2F_{7/2}$ state to the $^2F_{5/2}$ state. The excited Yb^{3+} ions transfer its absorbed energy to the neighboring Er^{3+} ion and excite it from the $^4I_{15/2}$ to the $^4I_{11/2}$, and then to the $^4F_{7/2}$ state. Alternatively, the energy transfer process

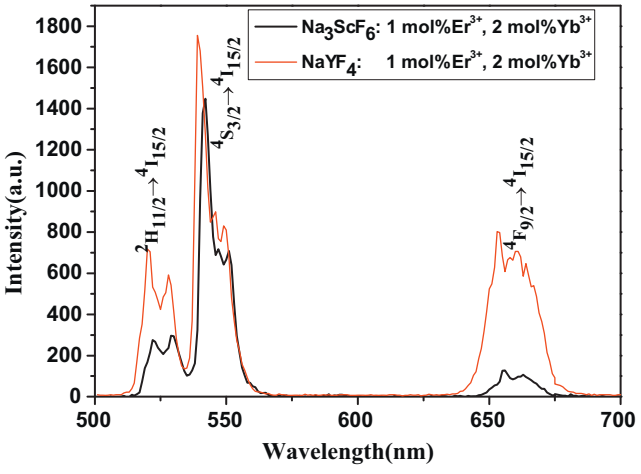

Fig. 4. UC photoluminescence (PL) spectra of Na_3ScF_6:1 mol% Er^{3+}, 2 mol% Yb^{3+} and $NaYF_4$:1 mol% Er^{3+}, 2 mol% Yb^{3+} microcrystals, respectively.

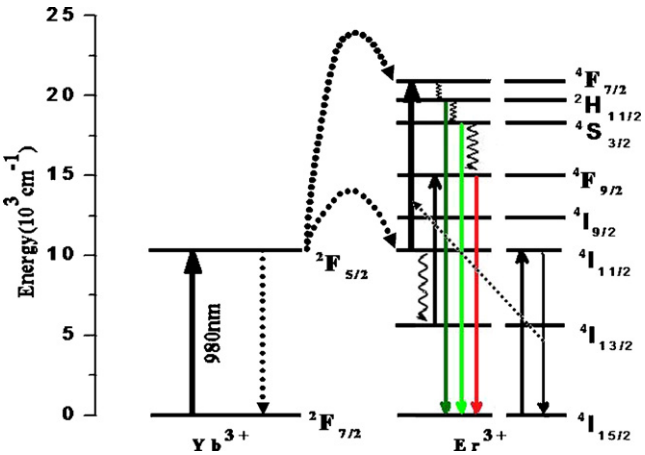

Fig. 6. The energy level diagrams of Yb^{3+} and Er^{3+} ions as well as the proposed UC mechanisms.

$^4I_{11/2} + {}^4I_{11/2} \rightarrow {}^4I_{15/2} + {}^4F_{7/2}$ or the excited state absorption process $^4I_{11/2} + h\nu \rightarrow {}^4F_{7/2}$ can also populate the $^4F_{7/2}$ levels. Multiphonon assisted relaxations from the $^4F_{7/2}$ state can then populate the $^2H_{11/2}$ and $^4S_{3/2}$ levels and generate the 525 and 540 nm emissions, respectively. The red emission at 660 nm originates from the $^4F_{9/2} \rightarrow {}^4I_{15/2}$ transition and the $^4F_{9/2}$ state can be populated based on nonradiative relaxations from the $^4S_{3/2}$ level and energy transfer from Yb^{3+}ions. The energy gap between the $^4S_{3/2}$ and $^4F_{9/2}$ level is about 2500 cm^{-1}, which requires at least 7 lattice phonons (phonon cut off energy of Na_3ScF_6:Er^{3+}/Yb^{3+} < 400 cm^{-1}). Therefore, the nonradiative relaxation rate is quite low. The energy transfer from Yb^{3+}ions can resonantly promote the Er^{3+} ion at the $^4I_{13/2}$ state to the $^4F_{9/2}$ state, i.e., $^4I_{13/2}(Er) + {}^4F_{5/2}(Yb) \rightarrow {}^4F_{9/2}(Er) + {}^4F_{7/2}(Yb)$. The $^4I_{13/2}$ state is populated by nonradiative relxations from the $^4I_{11/2}$ sate, which involves about also 9 lattice phonons to bridge the large energy gap of about ~3600 cm^{-1} [37]. Since both the two pathways are hard to occur, this therefore leads to a low red UC emission and in good agreement with the experimental observations in Fig. 3.

4. Conclusions

In summary, monoclinic Na_3ScF_6:1 mol% Er^{3+}, 2 mol% Yb^{3+} microcrystals have been successfully synthesized by a facile hydrothermal approach. The samples display high uniformity and crystallization with an average size of 1 μm in length. In addition, intense green UC emissions were observed in Na_3ScF_6:1 mol% Er^{3+}, 2 mol% Yb^{3+} powders under the excitation of 980 nm, and the mechanism of the observed UC emissions are proposed. This work provides a simple and facile approach to synthesize the monoclinic Na_3ScF_6:1 mol% Er^{3+}, 2 mol% Yb^{3+}, which might have great impact in practical applications.

Acknowledgment

This work is supported by Natural Science Foundation of China (51102066).

References

[1] S. Ghosh, T.F. Rosenbaum, G. Aeppli, S.N. Coppersmith, Nature 425 (2003) 48.
[2] F. Wang, Y. Han, C.S. Lim, Y.H. Lu, J. Wang, J. Xu, H.G. Chen, C. Zhang, M.H. Hong, X.G. Liu, Nature 463 (2010) 1061.
[3] E. Downing, L. Hesselimk, J. Ralston, R. Macfarlane, Science 273 (1996) 1185.
[4] G.H. Yi, H.C. Lu, S.Y. Zhao, G. Yue, W.J. Yang, D.P. Chen, L.H. Guo, Nano Lett. 4 (2004) 2191.
[5] L.Y. Wang, Y.D. Li, Chem. Commun. 24 (2006) 2557.
[6] H. Chen, X.S. Zhai, D. Li, L.L. Wang, D. Zhao, W.P. Qin, J. Alloys Compd. 511 (2012) 70–73.
[7] A. Shalav, B.S. Richards, T. Trupke, K.W. Krämer, H.U. Güdel, Appl. Phys. Lett. 86 (2005) 013505.
[8] J. de Wild, A. Meijerink, J.K. Rath, W.G.J.H.M. van Sark, R.E.I. Schropp, Energy Environ. Sci. 4 (2011) 4835.
[9] R.S. Khnayzer, J. Blumhoff, J.A. Harrington, A. Haefele, F. Deng, F.N. Castellano, Chem. Commun. 48 (2012) 209.
[10] J.W. Stouwdam, F.C. van Veggel, Nano Lett. 2 (2002) 733.
[11] R.X. Yan, Y.D. Li, Adv. Funct. Mater. 15 (2005) 763.
[12] C.M. Bender, J.M. Burlitch, Chem. Mater. 12 (2000) 1969.
[13] J.F. Suyver, J. Grimm, K.W. Krämer, H.U. Güdel, Luminescence 114 (2005) 53.
[14] J.F. Suyver, J. Grimm, K.W. Krämer, H.U. Güdel, Luminescence 117 (2006) 1.
[15] J.A. Capobianco, F. Vetrone, L.A. Cuccia, J.C. Boyer, J. Am. Chem. Soc. 128 (2006) 7444.
[16] N. Martin, P. Boutinaud, R. Mahiou, J. Cousseins, M. Bouderbala, J. Mater. Chem. 9 (1999) 125.
[17] Y.W. Zhang, X. Sun, R. Si, L.P. You, C.H. Yan, J. Am. Chem. Soc. 127 (2005) 3260.
[18] G.S. Yi, G.M. Chow, Chem. Mater. 19 (2007) 341.
[19] F. Wang, D.K. Chatterjee, Z.Q. Li, Y. Zhang, X.P. Fan, M.Q. Wang, Nanotechnology 17 (2006) 5786.
[20] C.F. Xu, M. Ma, S.J. Zeng, G.Z. Ren, L.W. Yang, Q.B. Yang, J. Alloys Compd. 509 (2011) 7943–7947.
[21] Q. X.S., X.P. Fan, Z. Xue, X.H. Xu, Q. Luo, J. Alloys Compd. 509 (2011) 4714–4721.
[22] Q. Sun, X.Q. Chen, Z.K. Liu, F.P. Wang, Z.H. Jiang, C. Wang, J. Alloys Compd. 509 (2011) 5336–5340.
[23] Y.L. Song, Q.W. Tian, R.J. Zou, Z.G. Chen, J.M. Yang, J.Q. Hu, J. Alloys Compd. 509 (2011) 6539–6544.
[24] Q. Liu, Y. Sun, T.S. Yang, W. Feng, C.G. Li, F.Y. Li, J. Am. Chem. Soc. 133 (2011) 17122.
[25] Q.Q. Dou, Y. Zhang, Langmuir 27 (2011) 13236.
[26] R. Naccache, F. Vetrone, V. Mahalingam, Chem. Mater. 21 (2009) 717.
[27] C.H. Liu, H. Wang, X.R. Zhang, J. Mater. Chem. 19 (2009) 489.
[28] C.T. Xu, J. Axelsson, S. Andersson-Engels, Appl. Phys. Lett. 94 (2009) 251107.
[29] G.Z. Ren, S.J. Zeng, J.H. Hao, J. Phys. Chem. C 115 (2011) 20141–20147.
[30] F. Wang, R.R. Deng, J. Wang, Q.X. Wang, Y. Han, H.M. Zhu, X.Y. Chen, X.G. Liu, Nat. Mater. 10 (2011) 968.
[31] G.Y. Chen, T.Y. Ohulchanskyy, A. Kachynski, H. Agren, P.N. Prasad, ACS Nano 6 (2011) 4981.
[32] A.K. Tyagia, J.K. Hlerb, P. Balogb, J. Weber, J. Solid State Chem. 178 (2005) 2620–2625.
[33] F. Wang, X.G. Liu, Chem. Soc. Rev. 38 (2009) 976.
[34] M. Haase, H. Schafer, Angew. Chem. Int. Ed. 50 (2011) 5808.
[35] Q.M. Huang, J.C. Yu, E. Ma, K.M. Lin, J. Phys. Chem. C 114 (2010) 4719–4724.
[36] W. Song, A.E. Vasdekis, Z. Li, D. Psaltis, Appl. Phys. Lett. 94 (2009) 051117.
[37] J.W. Zhao, Y.J. Sun, X.G. Kong, L.J. Tian, Y. Wang, J. Phys. Chem. B 112 (2008) 15666–15672.